Journal of Physics: Condensed Matter

OPEN ACCESS

RECEIVED
16 September 2025

REVISED
2 December 2025

ACCEPTED FOR PUBLICATION
23 December 2025

PUBLISHED
29 January 2026

PAPER

Resonances crossing in double-well quantum systems*

Andrea Sacchetti**

Department of Physics, Informatics and Mathematics, University of Modena e Reggio Emilia, Modena, Italy
**Author to whom any correspondence should be addressed.

E-mail: andrea.sacchetti@unimore.it

Keywords: quantum resonances for Schrödinger's equation, resonant tunnellig effect, time decay of quantum systems, quantum sensors of a DC electric field

Abstract

When the energy levels of a double-well system are nearly aligned, a beating motion occurs between the two wells. However, in the case of quantum resonances this scenario is much more intricate because in the complex plane two different types of resonance crossings (RCs) there exist, and beating motion occurs in only one of them. In this paper we use a quantitative criterion to determine whether the parameters of the quantum system are associated with one type of RC or the other. This analysis is essential for designing a quantum sensor made by heterostructures that easily and quickly measures whether an electric field has a predefined intensity.

1. Introduction

It is known that in a double-well system, when the energy levels are nearly aligned, a wave packet prepared within one of the two wells will oscillate between the two wells due to the resonance tunneling effect, and the oscillation period is given by the inversion of the splitting of the energy levels (see section 8.5 [1]). It is thus a sort of quantum sensor with basically two outputs: the beating motion of some physical observable, e.g. the *survival amplitude*, between the two wells when a pair of energy levels is aligned or no significant oscillation otherwise.

The typical model of such a quantum sensor consists of an internal (or unperturbed) asymmetric double-well Hamiltonian under the effect of a Stark potential dues to a DC electric field. The basic idea is that the DC electric field produces a change in energy levels, and when the electric field strength reaches a predefined value such that two energy levels cross, a periodic beating motion between the two wells occurs. Therefore, it is possible to check whether the intensity of the DC electric field is close to the predefined value simply by observing the presence or absence of such a beating motion. The advantage of this device is its simplicity and speed of response in order to check whether the strength of the DC electric field falls within a certain range, without the need to measure its period as in quantum sensors based on the Ramsey interferometer [2] (see also [3] and the references therein).

The applications of such a quantum sensor can be many; we can mention a couple of them as examples. For example, it checks very quickly and easily whether the charge value of a nano-battery [4] becomes lower (or higher, while charging the battery) than a given value. Also in medical diagnostics, this device could find application in encephalography [5] to monitor the presence/absence of electrical activity.

A first attempt to propose such a device has recently been discussed [6] in a toy model where the two wells are modeled by attractive Dirac's δ. To go beyond this toy model and develop a realistic model, we can consider the case in which the two wells are realised by heterostructures as explained by [7], see also [8]. Experiments with heterostructures began to be performed since the 70s; in one of these

* Andrea Sacchetti is member of Gruppo Nazionale per la Fisica Matematica of Istituto Nazionale: di. Alta Matematica (GNFM-INdAM). This work is partially supported by the Next Generation EU—Prin 2022CHELC7 project 'Singular Interactions and Effective Models in Mathematical Physics' and the UniMoRe-FIM project 'Modelli e metodi della Fisica Matematica'.

experiments a clear evidence was given for the resonant tunnel effect between barriers [9]. In later years, this type of experiment was greatly expanded considering also the case where an external electric field applied to the heterostructures is present; in such a case the most relevant phenomenon is the resonant tunnel effect between the two wells through the barrier for critical values of the strength of the electric field. For instance, we just name a few of the many experimental works devoted to the study of the resonant tunneling effect between symmetric or asymmetrical coupled quantum wells for different values of the heterostructure GaAs/AlGaAs parameters [10–16]; in particular, to the analysis of coherent oscillations of a wave packet in double-well structure [17] and to the study of the dependence of resonant tunneling times between quantum wells on barrier thickness [18]. This line of experimental research is still very active, as demonstrated by recent works [19, 20].

The analytical study of the crossing of bound states as the electric field strength varies was analysed for a GaAs/AlGaAs heterostructure (see section 3.13 [8] for numerical results, and also [21] for a review and [22] when the double-well potential is confining). In fact, no bound states are allowed when the electric field is turned on, but quantum resonances with a non-zero imaginary part that substantially determines the time dynamics of physical observable occur. It should be emphasised that in the above quoted papers the phenomenon of resonant crossing is not analysed in its entirety because the kind of crossing depends not only on the internal barrier but it depends on the external barrier due to the electric field, too. This fact has important implications because, as we will show later, the phenomenon of resonances crossing is not always associated with beating motion, which is the cornerstone of above mentioned quantum sensor. A detailed phenomenological characterisation of the different types of resonances crossing was provided [23] (see also the numerical experiments in tilted symmetric [24] and asymmetrical [25, 26] double-well structures), but without giving quantitative results; a similar study was also carried out by [27] where the two wells were modeled using attractive Dirac's deltas. Finally, in the case of double-well potentials, we mention also two recent theoretical researches on the analysis of quantum tunneling in the dynamical systems framework [28] and on the dependence of the switch rate from the barrier thickness [29].

Since previous studies have not used quantitative tools to establish the nature and behaviour of quantum resonances and the properties of the associated metastable states, it emerges that a more comprehensive analysis is therefore needed, and in this paper we take a significant step toward a deeper understanding of quantum resonances in tilted double-well (TDW) systems. More specifically, in this work we apply a criterion, introduced in a general setting by [30, 31] and recently used by [6] in a toy model, for analysing the nature of resonances crossing in a realistic TDW model based on heterostructures; not only that, we also explores in depth for the first time the relationship between the nature of resonance crossings (RCs) and the symmetry properties of the associated metastable states. As a result, the theoretical foundation for the design of quantum sensors based on this effect follows.

Even if we restrict our analysis to tilted double square well potentials we point out that this analysis can be extended, in principle, to the case where the two wells have different shapes; however, in this case, the calculation of the intersection point is much more difficult from a computational point of view, as well as the calculation of Agmon distances discussed in section A.3. Also the extension to tilted multiple-well may be considered, provided that, in addition to these difficulties, it is taken into account the semiclassical analysis developed in [32] for multiple-well problems.

The paper is organised as follows: in section 2 we introduce and describe the mathematical dimensionless model of the TDW, with special emphasise in section 2.1 to the analysis of the resonances crossing; section 2.2 is devoted to the analysis of the dynamics of the survival amplitude in a numerical experiment. In section 3 we consider a proposal for a quantum sensor based on a TDW, the values of the parameters are of order of the ones considered in typical experiments, and the dimensionless Hamiltonian corresponds to the one studied in the previous section. In section 4 we collect some conclusions. Eventually, an appendix is added where some technical results concerning Quantum resonances (section A.1), Localisation of the metastable states (section A.2) and Agmon's lenght (section A.3) are collected.

2. Methods

We now consider the one-dimensional Hamiltonian

$$H = -\frac{\mathrm{d}^2}{\mathrm{d}x^2} + V_{\alpha_1,\alpha_2}(x) - Fx, \tag{2.1}$$

in dimensionless units such that $2m = 1$, $\hbar = 1$ and $e = 1$ (where e is the electron charge), where the potential $V_{\alpha_1,\alpha_2} - Fx$ has a TDW shape (see equation (2.4) and figure 1). It has no eigenvalues and we

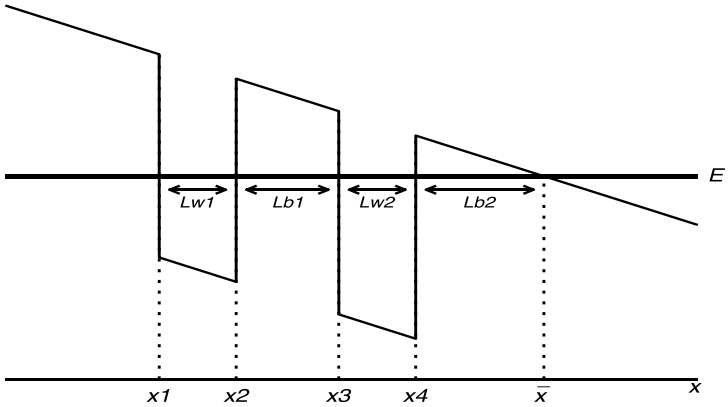

Figure 1. Plot of the tilted double square well potential. The internal barrier between the two wells is (x_2, x_3), and for a given value E of the energy the external barrier is $(x_4, \bar{x})$, $\bar{x} = -E/F$.

assume, for argument's sake, that it admits only two *sharp* quantum resonances E_1 and E_2 (by sharp resonance we mean a quantum resonance whose imaginary part is, in absolute value, very small) with associated metastable states ψ_1 and ψ_2. The energy levels of these two resonances depend on the strength F of the electric field and, for a suitable value of such a parameter, we can make the two quantum resonances closer and closer. We recall that the imaginary part of a quantum resonance is strictly negative. Two different kinds of RC may occur:

- Type *I* RC when there is an exact crossing of the imaginary parts of the resonances and an avoided crossing of their real parts;
- Type *II* RC when there is an exact crossing of the real parts of the resonances and an avoided crossing of their imaginary parts.

Only in exceptional cases, for very particular values of the model's parameters, the exact intersection of the two resonances may occur.

The dynamics of physical observable can be described by means of quantum resonances. For instance, the *survival amplitude* defined as

$$\mathcal{A}(t) = \langle \psi_0, \mathrm{e}^{-\mathrm{i}tH/\hbar}\psi_0 \rangle, \tag{2.2}$$

where ψ_0 is the initial state at the instant t_0 (for the sake of simplicity we may always assume that $t_0 = 0$ and $\langle \cdot, \cdot \rangle$ denotes the scalar product in $L^2(\mathbb{R}, \mathrm{d}x)$), has dominant term for intermediate times given by (see formula (A.2) in appendix A.1)

$$\mathcal{A}(t) \sim \sum_{j=1}^{2} c_{E_j} \mathrm{e}^{-\mathrm{i}tE_j/\hbar}, \tag{2.3}$$

where the coefficients c_{E_j} depend on the initial wavefunctions ψ_0, because H has only two sharp resonances E_1 and E_2. When the imaginary parts of the two resonances E_j are quite close each other and the coefficients c_{E_j} are both quite different from zero then an interference effect is triggered in (2.3) and, as a result, $\mathcal{A}(t)$ exhibits an oscillating damped behaviour with a *pseudo-period* given by $T = 2\pi\hbar/\omega$ where $\omega = |\Re E_2 - \Re E_1|$. Otherwise, $\mathcal{A}(t)$ exponentially decays without significant oscillations. Therefore, we expect to see large oscillations of the survival amplitude only in the occurrence of RC of type *I* because at the crossing point $\Im E_1 = \Im E_2$.

2.1. Resonances crossing criterion

In order to quantitatively study the RC in an explicit model we consider the double-well potential with square wells

$$V_{\alpha_1,\alpha_2}(x) = \begin{cases} 0 & \text{if } x < x_1 := 0 \\ \alpha_1 & \text{if } x_1 < x < x_2 := x_1 + L_{\mathrm{w}_1} \\ 0 & \text{if } x_2 < x < x_3 := x_2 + L_{\mathrm{b}_1} \\ \alpha_2 & \text{if } x_3 < x < x_4 := x_3 + L_{\mathrm{w}_2} \\ 0 & \text{if } x_4 < x \end{cases}, \tag{2.4}$$

under the effect of an external homogeneous electric field with strength F. Here, for the sake of definiteness, we set $x_1 = 0$ and $F > 0$. When $\alpha_1, \alpha_2 < 0$ then the potential has two wells with lengths L_{w_1} and L_{w_2} and for energies E in the range $(-Fx_1 + \alpha_1, -Fx_4)$ two barriers occur: one *internal* (or *inner*) barrier, between the two wells, with length L_{b_1} and another one is *external* (or *outer*) with length L_{b_2} depending on the value of the electric field strength F (see figure 1).

We consider, for argument's sake, the case where $\alpha_1 = \alpha_2$ and where the first well is larger than the second one, i.e. $L_{w_1} > L_{w_2}$; hence, for $F = 0$ the double-well operator H has two real-valued eigenvalues $E_1 < E_2 < 0$ where the ground state wavefunction ψ_1 associated to E_1 is mostly localised within the left-hand side well, while the second wavefunction ψ_2 associated to E_2 is mostly localised within the right-hand side well.

When we vary the parameter F and it takes strictly positive values then the spectrum of H is purely essential and it coincides with the whole real axis, i.e. $\sigma(H) = \sigma_{ess}(H) = \mathbb{R}$; therefore, the discrete spectrum is empty and there are no eigenvalues and the two former eigenvalues E_1 and E_2 obtained when $F = 0$ switch to sharp resonances and, for a critical value for F, they cross.

Quantum resonances are computed here looking for solutions to equation $H\psi = E\psi$, where $\Im E < 0$, with matching conditions

$$\psi(x) \text{ and } \frac{\mathrm{d}\psi(x)}{\mathrm{d}x} \text{ continuous at } x_n,\ n = 1, 2, 3, 4, \tag{2.5}$$

outgoing condition $\psi(x) \to 0$ as $x \to -\infty$ and the Siegert's outgoing condition [33, 34] that, in the case of Stark potential, takes the form [27, 35]

$$\psi(x) = B_i(\zeta) + \mathrm{i}A_i(\zeta), \text{ as } x \to +\infty; \tag{2.6}$$

where $\zeta = -(Fx + E)/F^{2/3}$ and A_i and B_i are the Airy functions.

In order to study the kind of crossing we introduce the two single well operators

$$H_j = -\frac{\mathrm{d}^2}{\mathrm{d}x^2} + V_j - Fx, \tag{2.7}$$

where $V_1 = V_{\alpha_1,0}$ and $V_2 = V_{0,\alpha_2}$ are single well potentials obtained by filling one of the two wells. Let μ_j be the ground state resonance of H_j and let F_C be the value of F such that $\mu := \Re\mu_1 = \Re\mu_2$. Then, when we consider the TDW problem (2.1) the two resonances E_1 and E_2 will cross at a value, denoted by f_C, close to F_C. For $F = F_C$ let ρ_i be the Agmon's length (defined in appendix A.3) of the internal barrier at energy μ and let ρ_e be the Agmon's length of the external one; then semiclassical analysis predicts that we have a RC of type *I* when $\rho_i < 2\rho_e$, and a RC of type *II* when $\rho_i > 2\rho_e$. We must emphasise that such a semiclassical result, obtained in the limit $\hbar \ll 1$, still holds true also in numerical experiments where $\hbar$ has a fixed value [36].

Concerning the metastable states ψ_j of H associated to the quantum resonances E_j we also find that in the case of quantum crossing of type *I* with F close to the crossing point F_C they are equally localised within both two wells; otherwise, the first metastable state is mostly localised within just one well while the second one is mostly localised within the other well.

This result is rather important, and it holds true in a general TDW model (see appendix A.2 for details). In conclusion, we can state that:

Proposition 1. *Let H be a one-dimensional Schrödinger operator with a TDW potential with two sharp resonances. Then:*
(A) In the case of RC of kind I with F close to F_C the imaginary parts of the two resonances are very close to each other, and the associated metastable states ψ_1 and ψ_2 are equally localised within the two wells.
(B) Otherwise, that is, in the case of RC of type I with F sufficiently far from F_C or in the case of RC of type II, the imaginary parts of the two resonances are rather different from each other; moreover, one of the associated metastable states is localised within just one of the two wells, and the other metastable state is localised within the other well.

As a comment to the above Proposition we can state that the exact crossing of the imaginary part of the two resonances is associated to the symmetry of the two metastable states; this result, which is well known in the case of symmetrical double-well potentials, is here extended to the case of asymmetrical potentials.

Here, we consider a numerical experiment with the following data in dimensionless units: $\alpha_1 = \alpha_2 = -0.264(4) \cdot 10^{-2}$; the left-hand side well has length $L_{w_1} = 60$; the right-hand side well has length $L_{w_2} =$

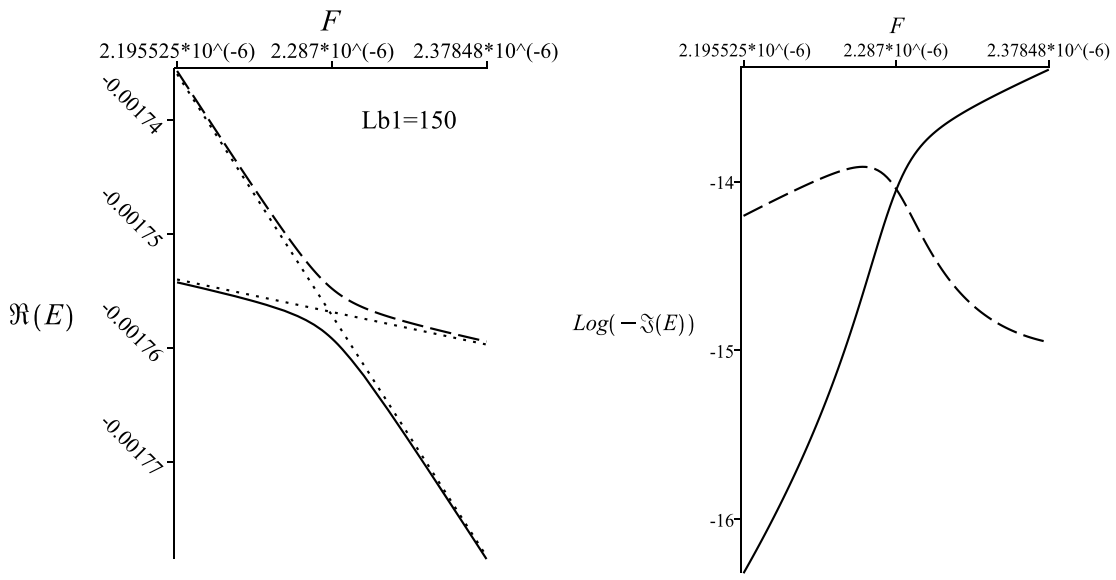

Figure 2. Here we plot the real parts (left-hand side panel) and the imaginary parts (right-hand side panel) of the two resonances E_1 (full line) and E_2 (broken line) of H in the case of internal barrier length $L_{b_1} = 150$ in dimensionless units; dot lines correspond to the real parts of the two resonances μ_1 and μ_2 of the single well operators (2.7). Dot lines cross at $F_C = 0.228(6) \cdot 10^{-5}$; the imaginary parts of the two resonances cross at $f_C = 0.228(7) \cdot 10^{-5}$. We observe a type I crossing where we have an avoided crossing of the real parts of the two resonances and an exact crossing of their imaginary parts.

40; the internal barrier has length $L_{b_1} = 150$. When $F = 0$ then H has two eigenvalues

$$E_1 = -0.168\,(7) \cdot 10^{-2} < E_2 = -0.123\,(0) \cdot 10^{-2}\,. \tag{2.8}$$

When we switch on the external electric field, i.e. for $F > 0$, then the general solution to equation $H\psi = E\psi$ is given by

$$\psi\,(x) = \begin{cases} aA_i\,(\zeta) + bB_i\,(\zeta) & \text{if } x \le x_1 \\ cA_i\,(\zeta_1) + dB_i\,(\zeta_1) & \text{if } x_1 < x < x_2 \\ eA_i\,(\zeta) + fB_i\,(\zeta) & \text{if } x_2 \le x \le x_3 \\ gA_i\,(\zeta_2) + hB_i\,(\zeta_2) & \text{if } x_3 < x < x_4 \\ \ell A_i\,(\zeta) + mB_i\,(\zeta) & \text{if } x_4 \le x \end{cases}.$$

where $\zeta_j = -(Fx + E - \alpha_j)/F^{2/3}$, $j = 1, 2$, then the outgoing conditions (2.6) implies that $b = 0$ and $\ell = im$, for some $m \neq 0$. We then impose the validity of the matching conditions (2.5) and finally solve the resulting equation for different values of F; in such a way we can compute the two quantum resonances as function of the electric field strength and we can observe the occurrence of a type I crossing when F runs in a neighbourhood of F_C (see figure 2).

In fact, the value of F at which the two single well resonances μ_1 and μ_2 of, respectively, H_1 and H_2 have the same real part is $F_C = 0.228(6) \cdot 10^{-5}$, and at this value we have that $\mu = -0.175(7) \cdot 10^{-2}$; the value f_C for which the imaginary parts of the quantum resonances E_1 and E_2 of H exactly cross is given by $f_C = 0.228(7) \cdot 10^{-5}$. The ratio between the Agmon's distances is (see appendix A.3)

$$\frac{\rho_i}{2\rho_e} = 0.239\,(7) < 1\,,$$

in agreement with the fact that we have a type I crossing.

2.2. Analysis of the survival amplitude

Concerning the time behaviour of the survival amplitude $\mathcal{A}(t) = \langle \psi_0, e^{-iHt}\psi_0 \rangle$ we stress that it depends on the kind of RC. In fact, in the TDW model considered in the previous section, where we have only two sharp resonances E_1 and E_2, the behaviour of the survival amplitude is expected to be given, at intermediate times, by formula (2.3). Since both resonances have a strictly negative imaginary part, we expect to observe a damped behaviour of the survival amplitude.

In the case (A) we have that $\Im E_1 \approx \Im E_2$ when F is close to F_C and, therefore, a damped oscillating behaviour due to the interference between the two metastable states occurs.

Table 1. table of values of the quantum resonances E_j and of the coefficients c_{E_j}, $j = 1, 2$, for different values of F; this model corresponds to a type I crossing where $L_{b_1} = 150$ and the critical value is $F_C = 0.288(7) \cdot 10^{-5}$. Here $F_\gamma = [1 + \gamma/100]F_C$.

F	F_{-4}	F_{-2}	F_C	F_2	F_4
$\Re E_1$	$-0.175(4) \cdot 10^{-2}$	$-0.175(6) \cdot 10^{-2}$	$-0.175(9) \cdot 10^{-2}$	$-0.176(8) \cdot 10^{-2}$	$-0.177(9) \cdot 10^{-2}$
$\Im E_1$	$-0.465(6) \cdot 10^{-16}$	$-0.387(5) \cdot 10^{-15}$	$-0.848(3) \cdot 10^{-14}$	$-0.273(9) \cdot 10^{-13}$	$-0.459(0) \cdot 10^{-13}$
$\Re E_2$	$-0.173(5) \cdot 10^{-2}$	$-0.174(6) \cdot 10^{-2}$	$-0.175(5) \cdot 10^{-2}$	$-0.175(8) \cdot 10^{-2}$	$-0.175(9) \cdot 10^{-2}$
$\Im E_1$	$-0.624(8) \cdot 10^{-14}$	$-0.103(5) \cdot 10^{-13}$	$-0.942(9) \cdot 10^{-14}$	$-0.191(4) \cdot 10^{-14}$	$-0.113(4) \cdot 10^{-14}$
T			$0.143(6) \cdot 10^{7}$		
$\Re c_{E_1}$	0.987(0)	0.951(7)	0.494(6)	$0.492(7) \cdot 10^{-1}$	$0.141(1) \cdot 10^{-1}$
$\Im c_{E_1}$	$-0.367(4) \cdot 10^{-9}$	$-0.149(4) \cdot 10^{-8}$	$-0.366(1) \cdot 10^{-8}$	$-0.238(4) \cdot 10^{-9}$	$-0.509(3) \cdot 10^{-10}$
$\Re c_{E_2}$	$0.134(4) \cdot 10^{-1}$	$0.490(4) \cdot 10^{-1}$	0.508(5)	0.951(5)	0.986(2)
$\Im c_{E_2}$	$0.117(0) \cdot 10^{-10}$	$0.121(4) \cdot 10^{-9}$	$0.458(6) \cdot 10^{-8}$	$0.731(1) \cdot 10^{-8}$	$0.842(5) \cdot 10^{-8}$

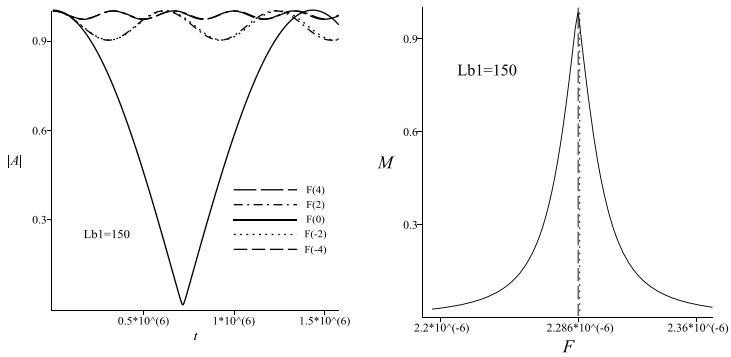

Figure 3. In the left-hand side panel we plot the graphs of $|\mathcal{A}(t)|$ for $F = F_{-4}, F_{-2}, F_C, F_2, F_4$; we see that large oscillations only occurs when F is close to F_C, the beating period is $T = 0.143(6) \cdot 10^7$ in dimensionless units. In the right-hand side panel we plot the value of the amplitude M of the beating motion when F runs in the interval $[F_{-4}, F_4]$. In this case the values of F_C (broken line) and f_C (dot line) are very narrow. Here $F_\gamma = [1 + \gamma/100]F_C$.

On the other hand, in case (B) we have that $\Im E_1$ is rather different from $\Im E_2$ and therefore one of the two terms e^{-itE_j} in (2.3) decays much faster than the other one; consequently, we expect to observe an exponential decay of $\mathcal{A}(t)$ without significant oscillations.

This scenario becomes more explicit when the initial state ψ_0 prepared within only one of the two wells is chosen. In fact, in this case the two coefficients c_{E_1} and c_{E_2} are of the same order in case (A) because the two metastable states ψ_1 and ψ_2 are equally localised within both wells; while in case (B) one of these coefficients is negligible because one of the two metastable states is localised within one well and the other is localised within the other well.

It should be noticed that in the experimental papers cited in the introduction it is implicitly assumed to be in case (A); but this is not necessarily always true. In fact, for different choices of model parameters, it is possible to fall into case (B) [36].

We now calculate the survival amplitude for the TDW model introduced in section 2.1 where we observe a RC of type I; the calculation of $|\mathcal{A}(t)|$ is performed using formula (2.3) and the initial wavefunction ψ_0 is prepared on the left-hand side well. We also represent the value of the amplitude of the oscillations

$$M := \max_t |\mathcal{A}(t)| - \min_t |\mathcal{A}(t)|,$$

as function of F.

In table 1 are collected the values of the quantum resonances E_j and of the coefficients c_{E_j}, $j = 1, 2$, for some values of F. We observe that when F is close enough to the value F_C then the imaginary parts of the two resonances E_1 and E_2 are very close to each other, and the two coefficients c_{E_1} and c_{E_2} are almost equal in absolute value; in such a case a beating motion is expected with beating (pseudo-)period given by $T = 2\pi/|\Re E_1 - \Re E_2|$. On the contrary, when F is not so close to F_C then the two imaginary parts of the resonances are very different and also one of the two coefficients is almost equal in absolute value to 1 while the other has a value close to 0; in such a case no wide oscillations are expected.

Therefore, a damped oscillating behaviour is observed in figure 3 for $|\mathcal{A}(t)|$ when the intensity F of the external field is close to F_C. Furthermore, the value of M reaches a maximum value at $F = F_C$ and, outside a small interval centred on F_C, it decreases rapidly.

In conclusion, we can state that for this choice of parameters, significant oscillations of the survival amplitude are observed when F is close to the predetermined value F_{C}, while for F outside the range $[F_{\mathrm{C}}-\delta_F, F_{\mathrm{C}}+\delta_F]$, where the δ_F is less than 4% of F_{C}, there are no significant oscillations. It should be noticed that a similar result is also obtained when the internal barrier is smaller, i.e. $L_{\mathrm{b}_1}=100$, or larger, i.e. $L_{\mathrm{b}_1}=200$; the difference is that in the former case δ_F is of order of 10%, while in the latter case it is of order of 2%.

3. Results

It is possible to design nanoscale devices that exhibit the characteristics described by the Hamiltonian (2.1). For example, we consider GaAs/AlGaAs heterostructures of the kind

$$\mathrm{Al}_s\mathrm{Ga}_{1-s}\mathrm{As}/\ell_{\mathrm{w}_1}\cdot\mathrm{GaAs}/\ell_{\mathrm{b}_1}\cdot\mathrm{Al}_s\mathrm{Ga}_{1-s}\mathrm{As}/\ell_{\mathrm{w}_2}\cdot\mathrm{GaAs}/\mathrm{Al}_s\mathrm{Ga}_{1-s}\mathrm{As}\,,$$

where $s\in(0,1)$, under the effect of a DC electric field perpendicular to the growth direction z of the heterostructure. Under the parabolic approximation of the band and in the envelope function approximation introduced in the 80s [37], see also [7, 8] for a review and [38, 39] for the mathematical justification, the Schrödinger equation reduces to a one-dimensional equation where the potential has a double square well shape under the effect of a Stark perturbation (see figure 1 in dimensionless units). We must emphasise that when we extend the model by adopting the Kane approximation of the band, then the steady states are now described by a fourth-order equation (see [40] and the references therein); we do not consider this case in the present work.

With more details, in the envelope function approximation the time independent Schrödinger equation takes the form $\mathcal{H}\psi=\mathcal{E}\psi$ where

$$\mathcal{H}=-\frac{\hbar^2}{2m^\star}\frac{\mathrm{d}^2}{\mathrm{d}z^2}+\mathcal{V}_{v_1,v_2}-e\mathcal{F}z,\ z\in\mathbb{R}\,, \tag{3.1}$$

where $m^\star$ is the effective mass of the electron, e is the electron charge and $\mathcal{F}$ is the strength of the electric field. In this framework we assume the validity of the time-dependent Schrödinger equation

$$\begin{cases} \mathrm{i}\hbar\frac{\partial\psi}{\partial\tau}=\mathcal{H}\psi \\ \psi\,(z,\tau)|_{\tau=0}=\psi_0\,(z) \end{cases}, \tag{3.2}$$

where $\psi_0(z)$ is the initial wave-function; in fact, ψ would be the envelope function (see section 7.6 [41], see also [42, 43]). The double square well potential has the form

$$\mathcal{V}_{v_1,v_2}\,(z)=\begin{cases} 0 & \text{if } z<z_1:=0 \\ v_1 & \text{if } z_1<z<z_2:=z_1+\ell_{\mathrm{w}_1} \\ 0 & \text{if } z_2<z<z_3:=z_2+\ell_{\mathrm{b}_1} \\ v_2 & \text{if } z_3<z<z_4:=z_3+\ell_{\mathrm{w}_2} \\ 0 & \text{if } z_4<z \end{cases},$$

where $v_1,v_2<0$, the two wells have lengths ℓ_{w_1} and ℓ_{w_2} and the *internal* (or *inner*) barrier has length ℓ_{b_1}. Typically, lengths of the wells ℓ_{w_j}, $j=1,2$, and of the barrier ℓ_{b_1} are of order of several tens of angstrom Å.

We consider here the simplest case where the effective electron mass in the wells coincides with the one in the barriers and is given by $m^\star=0.067m_0$ for the GaAs lattices (m_0 is the electron mass). In fact, such an approximation holds true provided that the parameter s is not too large, typically $s\leq 0.3$ (see figure 2.17 by [8]). A more refined model is to assume that the effective mass $m^\star=m^\star(z)$ depends on the spatial coordinate, then the matching conditions satisfy the so-called Ben-Daniel and Duke conditions (see section 2.6 by [8]), that is the continuity of ψ and of $\frac{1}{m^\star(z)}\frac{\mathrm{d}\psi}{\mathrm{d}z}$. However, in this paper, we do not dwell on the analysis of such matching conditions.

Let $\eta=1$ Å $=10^{-10}m$ and $\Lambda=\hbar^2/(2m^\star\eta^2)$ then equation (3.1) takes the dimensionless form (2.1) where

$$\mathcal{E}=\Lambda E,\ \mathcal{V}=\Lambda V,\ x_n=\frac{z_n}{\eta},\ n=1,2,3,4,\ \bar{x}=\frac{\bar{z}}{\eta},\text{and }\mathcal{F}=\frac{\Lambda}{\eta e}F.$$

Then, the lengths of the wells and barrier are, in dimensionless units, $L_{\mathrm{w}_j}=\eta^{-1}\ell_{\mathrm{w}_j}$, $j=1,2$, and $L_{\mathrm{b}_1}=\eta^{-1}\ell_{\mathrm{b}_1}$. Furthermore, equation (3.2) becomes

$$\begin{cases} \mathrm{i}\frac{\partial\psi}{\partial t} = H\psi \\ \psi(x,t)|_{t=0} = \psi_0(x) \end{cases},$$

where

$$t = \Lambda\tau/\hbar.$$

Concerning α_j, following the model proposed by section 3.9 [8] hereafter we assume, for the sake of definiteness, that $v_j = -165\,\mathrm{meV}$ (which corresponds to the case $s \approx 0.2$), then $\alpha_j = v_j/\Lambda = -0.264(4)\cdot 10^{-2}$.

When $F = 0$ then H has two eigenvalues (2.8) that correspond to

$$\mathcal{E}_1 = -95.9\,(3)\ \mathrm{meV} \text{ and } \mathcal{E}_2 = -69.9\,(4)\ \mathrm{meV}.$$

For $F > 0$ then these two eigenvalues switch to quantum resonances and the crossing point is around $F_{\mathrm{C}} = 0.228(6)\cdot 10^{-5}$; that is

$$\mathcal{F}_{\mathrm{C}} = \Lambda\eta^{-1}e^{-1}F_{\mathrm{C}} = 13.0\,(0)\ \mathrm{kV}\cdot\mathrm{cm}^{-1}.$$

We recall that the RC is of type *I*, see figure 2, in agreement with the fact that $\frac{\rho_{\mathrm{i}}}{2\rho_{\mathrm{e}}} = 0.239(7) < 1$. Finally, the beating pseudo-period at $\mathcal{F} = \mathcal{F}_{\mathrm{C}}$ is given by $\mathcal{T} = 0.166(3)\cdot 10^{-10}\,s.$ and the oscillations last for times of order $t \approx 10^{14}$, that is $\tau \approx 10^{-3}\,\mathrm{s}$.

4. Conclusions

The proposal device has the following feature: when the heterostructure with an internal barrier of length $\ell_{\mathrm{b}_1} = 150$ Å is perturbed by a DC electric field then, simply observing whether the survival amplitude has an oscillating behaviour or not, we can verify that the strength of the electric field is equal to $\mathcal{F}_{\mathrm{C}} = 13.0(0)\,\mathrm{kV}\cdot\mathrm{cm}^{-1}$ with a tolerance less than 4%.

The predefined value $\mathcal{F}_{\mathrm{C}}$ depends on the lengths of the inner barrier and of the two wells. Therefore, it is possible to design devices capable of measuring electric fields of any desired intensity by appropriately modulating the lengths and depths of the two wells and the length of the internal barrier. For instance, leaving the shape of the two wells unchanged, if the length of the internal barrier is $\ell_{\mathrm{b}_1} = 100$ Å then the device can check if the electric field strength is equal to $10.4(0)\,\mathrm{kV}\cdot\mathrm{cm}^{-1}$ with a tolerance less than 10%; while, if we change the length of the internal barrier to $\ell_{\mathrm{b}_1} = 200$ Å then the device can check if the electric field strength is equal to $17.3(3)\,\mathrm{kV}\cdot\mathrm{cm}^{-1}$ with a tolerance less than 2%. In both cases, the RC is of type *I*.

However, it is important to emphasise again that when projecting such a device one must be sure to have a RC of type *I*; otherwise, that is the model's parameters correspond to a RC of type *II*, then the beating behaviour of the survival amplitude is not triggered. This fact can be verified by calculating the Agmon's lengths of the barriers ρ_{i} and ρ_{e} and checking whether $\frac{\rho_{\mathrm{i}}}{2\rho_{\mathrm{e}}} < 1$; in fact, this theoretical criterion holds in the semiclassical limit $\hbar \ll 1$, but it has also been verified to be valid in realistic models [36]. This fact means that the range of validity of this device is determined by the condition $\rho_{\mathrm{i}} < 2\rho_{\mathrm{e}}$, where these two terms are given by formulas (A.13) and (A.14).

We close by underlining that our method sound to be quite robust with respect to perturbations. For instance, if we add a (relatively small) perturbation to the TDW potential in (3.1) then we actually expect the value $\mathcal{F}_{\mathrm{C}}$ of the intersection point to change slightly, but the dynamics of the survival amplitude maintains an unchanged behaviour in the vicinity of the new intersection point.

Data availability statement

All data that support the findings of this study are included within the article (and any supplementary files).

Competing of interests

The authors declare no competing interests.

Appendix

Here, we describe with more details some facts concerning quantum resonances and semiclassical results.

A.1. Quantum resonances

Quantum resonances constitute a mathematical model of metastable states: a resonance is a complex number whose real part is the rest energy of the state, and its imaginary part gives the rate of the decay of the state. If the system is described by the Hamiltonian (2.1) (where $2m=1$, $e=1$ and $\hbar=1$), the resonances are defined as the complex-valued poles of the meromorphic continuation of the kernel of the resolvent operator $[H-E]^{-1}$ from the half-plane $\Im E>0$ to the non-physical half-plane $\Im E<0$ (sometimes authors refer to $k=\sqrt{E}$ as a resonance). Equivalently, resonances may also be defined by means of the Siegert's outgoing conditions [33], see also [34] for a rigorous mathematical study of quantum resonances.

In their seminal paper [44] García–Calderón and Peierls discussed the possibility of expanding e^{-itH} in terms of the eigenvalues/resonances E of H and their associated eigenvectors/metastable states ψ_E. In particular, under suitable assumptions on the potential and if H has no resonances with zero energy, then the kernel $\mathcal{U}(x,y;t)$ of the evolution operator e^{-itH} is given by [45]

$$\mathcal{U}(x,y;t)=\sum_{\text{eigenvaluesE}}\mathrm{e}^{-\mathrm{i}tE}\psi_E(x)\,\psi_E(y)+ \\ +\sum_{\text{resonancesE}}\mathrm{e}^{-\mathrm{i}tE}\psi_E(x)\,\psi_E(y)+O\left(t^{-3/2}\right)\ \text{as}\ t\to+\infty\,, \tag{A.1}$$

where the resonant metastable states ψ_E associated to the resonances are normalised with respect to a suitable weighted norm and where the eigenfunctions ψ_E associated to the eigenvalues are normalised as usual, i.e. $\langle\psi_E,\psi_E\rangle=1$.

Suppose now to consider the time evolution of physical observable; for instance of the survival amplitude defined as (2.2). Thus, in absence of stable states the survival amplitude decreases in time because (A.1) takes the form

$$\mathcal{A}(t)=\sum_{\text{resonancesE}}c_E\mathrm{e}^{-\mathrm{i}tE}+O\left(t^{-3/2}\right)\,, \tag{A.2}$$

where

$$c_E=\langle\psi_0,\psi_E\rangle\,\langle\bar{\psi}_0,\psi_E\rangle\,. \tag{A.3}$$

This decay is, for a generic Hamiltonian without stable states, the contribution of different kinds of decay:

- for short times, that is in the so called quadratic Zeno region, the dominant term is a quadratic-type term [46];
- for intermediate times the dominant term is of exponential type and it is due to the decay effect associated with sharp resonances (that is with imaginary part small enough: $|\Im E|\ll 1$);
- for long times the dominant term is given by the power-law tail $O(t^{-3/2})$; in fact, when the potential is not bounded from below, like in TDW potentials, this term is absent.

A.2. Localisation of the metastable states

As pointed out in proposition 1, for a TDW model the metastable states associated to the quantum resonances E_j, $j=1,2$, are equally localised within both two wells in the case of RC of type I with F close enough to the crossing point F_{C}; otherwise, one metastable state is mostly localised within only one well and the other one is mostly localised within the other well. This fact can be seen in numerical experiments, see figure 4 where the two resonances E_1 and E_2 are calculated in table 1.

This fact can be understood by making use of some semiclassical results (that is obtained in the limit $h\to 0$ where we set $h:=\hbar/\sqrt{2m^\star}$) applied to Schrödinger operators (3.1), we refer to [30, 31] for details. Indeed, it is possible to prove that the calculation of the doublet of resonances of $\mathcal{H}$ can be reduced to the calculation of the two complex-valued eigenvalues of the 2×2 matrix

$$\begin{pmatrix}\lambda_1 & \beta\\ \beta & \lambda_2\end{pmatrix}+O(h^\infty)\,e^{-2\rho_{\mathrm{i}}/h},\ \text{as}\ h\to 0\,, \tag{A.4}$$

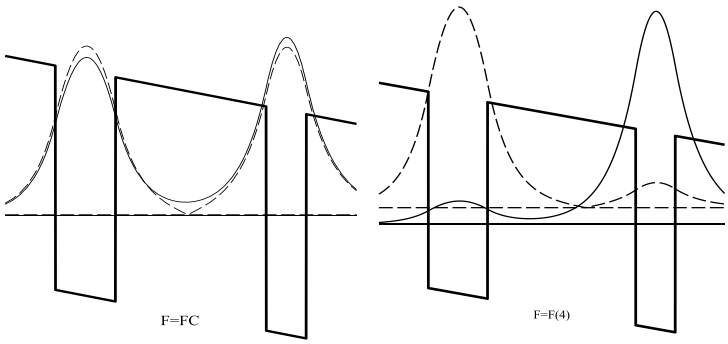

Figure 4. Here, we plot the potential (bold line), the energy levels $\Re E_1$ (full horizontal line) and $\Re E_2$ (broken horizontal line) and the absolute value of the metastable states $|\psi_1(x)|$ (full line) and $|\psi_2(x)|$ (broken line). In the left-hand side panel we are at the crossing point, that is $F = F_C$ where $\Re E_1$ and $\Re E_2$ are almost aligned, and the two metastable states are equally localised within both two wells; on the other hand, in the right-hand side panel we are slightly far from the crossing point, that is $F = F_4$, and it turns out that one metastable state is mostly localised within one well and the other metastable state is mostly localised within the other well.

where $\lambda_j = \Lambda\mu_j$ and where μ_j are the quantum resonances of the single well operators (2.7) and where $\beta = \tilde{\phi}e^{-\rho_i h}$ is a complex-valued coupling term, ρ_i is the Agmon's length of the internal barrier $[z_2, z_3]$, as defined in section 3 and $\tilde{\phi}$ is a quantity that satisfies

$$C^{-1}h^{-1/2} \leq |\tilde{\phi}| \leq Ch^{1/2}, \tag{A.5}$$

for some positive constant $C > 0$. Hence, the two quantum resonances are given, up to a small remainder term, by

$$\mathcal{E}_{1,2} \sim \frac{1}{2}(\lambda_1 + \lambda_2) \pm \sqrt{\frac{1}{4}(\lambda_1 - \lambda_2)^2 + \beta^2}, \text{ as } h \to 0. \tag{A.6}$$

At the crossing point where $\lambda := \Re\lambda_1 = \Re\lambda_2$ we have that the dominant terms of the imaginary parts of the single well resonances are given by

$$\Im\lambda_1 = -\tilde{\phi}_1 e^{-2(\rho_i+\rho_e)/h} \text{ and } \Im\lambda_2 = -\tilde{\phi}_2 e^{-2\rho_e/h}, \tag{A.7}$$

where ρ_e is the Agmon's length of the external barrier $[z_4, \bar{z}]$ as defined in section 3 and where $\tilde{\phi}_j$, $j = 1, 2$, are two positive real-valued quantities such that

$$C^{-1}h^{-1/2} \leq \tilde{\phi}_j \leq Ch^{1/2}, \ j = 1, 2. \tag{A.8}$$

In fact, the asymptotic behaviour of the single well resonances can be calculated by means of the WKB approximation as well, see, for instance, the papers [12, 18, 47]; to our purpouse we focus our attention on the exponential factors of the asymptotic behaviour. Hence,

$$\mathcal{E}_{1,2} \sim \lambda - \mathrm{i}\frac{1}{2}\tilde{\phi}_2 \mathrm{e}^{-2\rho_e/h} \pm \frac{1}{2}\sqrt{-\tilde{\phi}_2^2 e^{-4\rho_e/h} + \tilde{\phi}^2 \mathrm{e}^{-2\rho_i/h}}, \text{ as } h \to 0, \tag{A.9}$$

at the crossing point where $\lambda := \Re\lambda_1 = \Re\lambda_2$, and thus Proposition 1 follows. That is, RC of type *I* occurs when $2\rho_e > \rho_i$, and in this case the imaginary parts of the two resonances at the crossing point are of order $e^{-2\rho_e/h}$. For the same reason, it follows that a RC of type *II* occurs when $2\rho_e < \rho_i$.

In the case of RC of type *I*, in a neighbourhood of the crossing point where $\Re\lambda_1 = \Re\lambda_2$, the two eigenvectors w_j of the 2×2 matrix are given by

$$w_j \sim \begin{pmatrix} 1 \\ \frac{-\tilde{\phi}_2 \mathrm{e}^{-2\rho_e/h}}{2\tilde{\phi}\,\mathrm{e}^{-\rho_i/h}} - (-1)^j \sqrt{\frac{\tilde{\phi}_2^2 \mathrm{e}^{-2(2\rho_e-\rho_i)/h}}{4\tilde{\phi}^2} + 1} \end{pmatrix} \text{ as } h \to 0. \tag{A.10}$$

Hence, the *normalised* eigenvectors are given by $\frac{w_j}{|w_j|} \sim \begin{pmatrix} 1/\sqrt{2} \\ -(-1)^j/\sqrt{2} \end{pmatrix}$ as $h \to 0$, and this fact means that the two metastable states associated to the quantum resonances $\mathcal{E}_{1,2}$ are equally localised within both two wells. Otherwise, that is outside of such a neighbourhood or in the case of RC of type *II*, the

normalised eigenvectors of the matrix (A.4) have the asymptotic behaviours $\begin{pmatrix} 1 \\ 0 \end{pmatrix}$ and $\begin{pmatrix} 0 \\ 1 \end{pmatrix}$, which implies that one of the two metastable states is localised within one well, and the other metastable state is localised within the other well.

A.3. Agmon's length

The Agmon's distance in $\mathbb{R}^d$, where $d = 1, 2, 3, \ldots$ is the spatial dimension, computed at an energy λ is defined as the length of the geodesic path with metric $\sqrt{[V-\lambda]_+}dx$, dx is the standard metric in $\mathbb{R}^d$ and V is the potential (see section 3.2 [32] for details and further references).

In the case (3.1) the Agmon's lengths of the internal and external barriers are simply given by

$$\rho_{\rm i} = -\frac{2}{3\mathcal{F}_{\rm C}e}\left[(-\lambda - \mathcal{F}_{\rm C}ez)^{3/2}\right]_{z_2}^{z_3}, \tag{A.11}$$

and

$$\rho_{\rm e} = -\frac{2}{3\mathcal{F}_{\rm C}e}\left[(-\lambda - \mathcal{F}_{\rm C}ez)^{3/2}\right]_{z_4}^{\bar{z}}. \tag{A.12}$$

In conclusion, in the case (3.1) it follows that

$$\rho_{\rm i} = 0.430\,(2)\cdot 10^{-8}{\rm eV}^{1/2}\cdot{\rm m}, \tag{A.13}$$

and

$$\rho_{\rm e} = 0.897\,(3)\cdot 10^{-8}{\rm eV}^{1/2}\cdot{\rm m}. \tag{A.14}$$

ORCID iD

Andrea Sacchetti 0000-0001-6292-9251

References

[1] Merzbacher E 1998 *Quantum Mechanics* 3rd edn (Wiley)
[2] Ramsey N F 1950 *Phys. Rev.* **78** 695–9
[3] Degen C L, Reinhard F and Cappellaro P 2017 *Rev. Mod. Phys.* **89** 035002
[4] Vullum F, Teeters D, Nytèn A and Thomas J 2006 *Solid State Ion.* **177** 2833–8
[5] Aslam N, Zhou H, Urbach E K, Turner M J, Walsworth R L, Lukin M D and Park H 2023 *Nat. Rev. Phys.* **5** 157–69
[6] Sacchetti A 2024 *Phys. Scr.* **99** 105124
[7] Bastard G 1991 *Wave Mechanics Applied to Semiconductor Heterostructures* (Wiley)
[8] Harrison P 2005 *Quantum Wells, Wires and Dots: Theoretical and Computational Physics of Semiconductor Nanostructures* (Wiley)
[9] Chang L L, Esaki L and Tsu R 1974 *Appl. Phys. Lett.* **24** 593–5
[10] Oberli D Y, Shah J, Damen T C, Tu C W, Chang T Y, Miller D A B, Henry J E, Kopf R F, Sauer N and DiGiovanni A E 1989 *Phys. Rev. B* **40** 3028–31
[11] Matsusue T, Tsuchiya M, Schulman J N and Sakaki H 1990 *Phys. Rev. B* **42** 5719–34
[12] Nido M, Alexander M G W, Rühle W W, Schweizer T and Köhler K 1990 *Appl. Phys. Lett.* **56** 355–7
[13] Alexander M G W, Nido M, Rühle W W and Köhler K 1991 *Superlattices Microstruct.* **9** 83–86
[14] Leo K *et al* 1992 *IEEE J. Quantum Electron.* **28** 2498–507
[15] Shimizu N, Furuta T, Waho T and Mizutani T 1993 *Jpn. J. Appl. Phys.* **32** L306–8
[16] Ozaki S, Feng J M, Park J H, Osako S-I, Kubo H, Morifuji M, Mori N and Hamaguchi C 1998 *J. Appl. Phys.* **83** 962–5
[17] Leo K, Shah J, Göbel E O, Damen T C, Schmitt-Rink S, Schäfer W and Köhler K 1991 *Phys. Rev. Lett.* **66** 201–4
[18] Heberle A P, Zhou X Q, Tackeuchi A, Ruhle W W and Kohler K 1994 *Semicond. Sci. Technol.* **9** 519–22
[19] Zhu X, Bescond M, Onoue T, Bastard G, Carosella F, Ferreira R, Nagai N and Hirakawa K 2021 *Phys. Rev. Appl.* **16** 064017
[20] Philippe A, Carosella F, Zhu X, Salhani C, Hirakawa K, Bescond M, Ferreira R and Bastard G 2023 *J. Appl. Phys.* **134** 124305
[21] Ferreira R and Bastard G 1997 *Rep. Prog. Phys.* **60** 345–87
[22] Pedersen T G 2019 *Phys. Rev. B* **100** 155410
[23] Wagner M and Mizuta H 1993 *Phys. Rev. B* **48** 14393–406
[24] Sivalertporn K, Mouchliadis L, Ivanov A L, Philp R and Muljarov E A 2012 *Phys. Rev. B* **85** 045207
[25] Pandey L N and George T F 1991 *J. Appl. Phys.* **69** 2711–3
[26] Feng J M, Ozaki S, Park J H, Kubo H, Mori N and Hamaguchi C 1997 *Phys. Status Solidi b* **204** 412–5
[27] Korsch H J and Mossmann S 2003 *J. Phys. A: Math. Gen.* **36** 2139–53
[28] Ray S, Bhattacharyya S and Bhattacharjee J K 2025 *Phys. Lett. A* **532** 130174
[29] Su Q, Cortinas R G, Venkatraman J and Puri S 2025 *Phys. Rev. A* **112** 042202
[30] Grecchi V, Martinez A and Sacchetti A 1996 *J. Phys. A: Math. Gen.* **29** 4561–87
[31] Grecchi V, Martinez A and Sacchetti A 1996 *Asympt. Anal.* **13** 373–91
[32] Hellfer B 1988 *Semi-Classical Analysis for the Schrödinger Operator and Applications* (*Lecture Notes in Mathamatics* vol 1336) (Springer)
[33] Siegert A J F 1939 *Phys. Rev.* **56** 750–2
[34] Dyatlov S and Zworski M 2019 Mathematical Theory of Scattering Resonances *AMS - Graduate Studies in Mathematics* vol 200

[35] Juhasz D, Kolesik M and Jakobsen P K 2018 *J. Math. Phys.* **59** 113501
[36] Sacchetti A 2025 *Ann. Phys. (NY)* **480** 170122
[37] Bastard G 1981 *Phys. Rev. B* **24** 5693–7
[38] Burt G M 1992 *J. Phys.: Condens. Matter* **4** 6651–90
[39] Burt G M 1999 *J. Phys.: Condens. Matter* **11** 53–83
[40] Aliffi G E, Nastasi G and Romano V 2025 *Z. Angew. Math. Phys.* **76** 155
[41] Jacoboni C 2010 Theory of electron transport in semiconductors *A Path From Elementary Physics to Nonequilibrium Green Functions* (*Springer Series in Solid-State Sciences*) (Springer) p 165
[42] Muga J G and Cruz H 1992 *Physica B* **179** 326–34
[43] Cruz H and Muñoz A 1993 *Appl. Phys. A* **56** 40–42
[44] García-Calderón G and Peierls R 1976 *Nucl. Phys. A* **265** 443–60
[45] Albeverio S and Høegh-Krohn R 1984 The resonance expansion for the Green's function of the Schrödinger and wave equations *Resonances—Models and Phenomena* (*Lecture Notes in Physics* vol 211) ed S Albeverio, L S Ferreira and L Streit (Springer) pp 105–27
[46] Facchi P and Pascazio S 2008 *J. Phys. A: Math. Theor.* **41** 493001
[47] Capasso F, Mohammed K and Cho A 1986 *IEEE J. Quantum Electron.* **22** 1853–69